

Intravitreal Pharmacokinetic Study of the Antiangiogenic Glycoprotein Opticin

Eva M. del Amo, John R. Griffiths, Izabela P. Klaska, Justin Hoke, Anne White, Leon Aarons, Garth J. S. Cooper, James W. B. Bainbridge, Paul N. Bishop,* and Richard D. Unwin*



Cite This: *Mol. Pharmaceutics* 2020, 17, 2390–2397



Read Online

ACCESS |



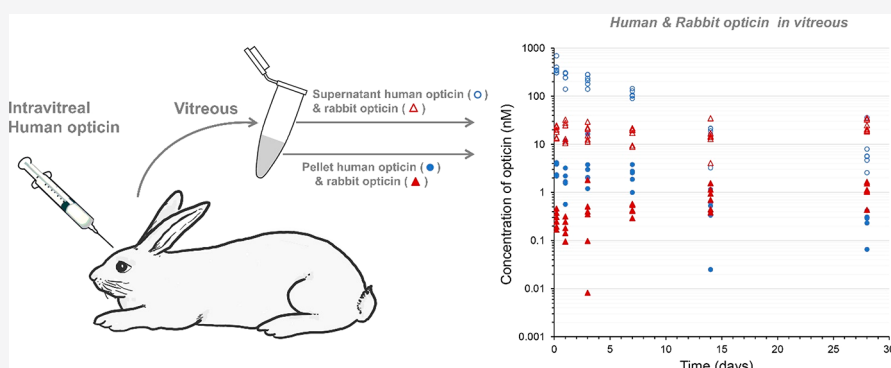
Metrics & More



Article Recommendations



Supporting Information



ABSTRACT: Opticin is an endogenous vitreous glycoprotein that may have therapeutic potential as it has been shown that supranormal concentrations suppress preretinal neovascularization. Herein we investigated the pharmacokinetics of opticin following intravitreal injection in rabbits. To measure simultaneously concentrations of human and rabbit opticin, a selected reaction monitoring mass spectrometry assay was developed. The mean concentration of endogenous rabbit opticin in 7 uninjected eyes was measured and found to be 19.2 nM or 0.62 $\mu\text{g}/\text{mL}$. When the vitreous was separated by centrifugation into a supernatant and collagen-containing pellet, 94% of the rabbit opticin was in the supernatant. Intravitreal injection of human opticin (40 μg) into both eyes of rabbits was followed by enucleation at 5, 24, and 72 h and 7, 14, and 28 days postinjection ($n = 6$ at each time point) and measurement of vitreous human and rabbit opticin concentrations in the supernatant and collagen-containing pellet following centrifugation. The volume of distribution of human opticin was calculated to be 3.31 mL, and the vitreous half-life was 4.2 days. Assuming that rabbit and human opticin are cleared from rabbit vitreous at the same rate, opticin is secreted into the vitreous at a rate of 0.14 $\mu\text{g}/\text{day}$. We conclude that intravitreally injected opticin has a vitreous half-life that is similar to currently available antiangiogenic therapeutics. While opticin was first identified bound to vitreous collagen fibrils, here we demonstrate that >90% of endogenous opticin is not bound to collagen. Endogenous opticin is secreted by the nonpigmented ciliary epithelium into the rabbit vitreous at a remarkably high rate, and the turnover in vitreous is approximately 15% per day.

KEYWORDS: opticin, intravitreal pharmacokinetics, selected reaction monitoring mass spectrometry, SLRP, neovascularization

INTRODUCTION

Opticin is an extracellular glycoprotein that was first identified bound to the surface of vitreous collagen fibrils.¹ It is a member of the small leucine-rich repeat proteoglycan/protein family (SLRP), and several other members of this family of extracellular matrix molecules are known to bind to collagen fibrils.² Opticin is extensively substituted with O-linked oligosaccharides and in solution exists as a homodimer (molecular weight of core protein and associated oligosaccharides being approximately 90 kDa) dimerizing through its leucine-rich repeat domains.³ It is synthesized by the nonpigmented ciliary epithelium and then secreted into the vitreous cavity.^{4–6} Immunohistochemical evidence suggests that opticin binds to the internal limiting membrane (ILM) on

the inner surface of the retina, and the ILM appears to impede the diffusion of opticin into the neurosensory retina which contains low levels.^{5,7} Functional work has demonstrated that opticin has antiangiogenic properties and that the underlying mechanism of action is interfering with endothelial cell adhesion to collagen.^{8,9} Studies using the murine oxygen-induced retinopathy model have shown that the antiangiogenic

Received: February 12, 2020

Revised: May 19, 2020

Accepted: May 21, 2020

Published: May 21, 2020



effects of opticin are dose-dependent: there was increased neovascularization in opticin null mice compared with wild-type controls, and when opticin was injected into the vitreous of wild-type mice, there was decreased neovascularization compared to carrier buffer injected controls.⁹ Therefore, increasing the amount of opticin in the vitreous cavity by injection of recombinant opticin could be an effective treatment for conditions characterized by preretinal neovascularization (growth of blood vessels into the vitreous), such as proliferative diabetic retinopathy and retinopathy of prematurity.

In this study, we aimed to measure the concentration of endogenous opticin in rabbit eyes and undertake pharmacokinetic (PK) studies to determine the PK properties of human opticin following intravitreal injection. To measure separately the concentrations of injected recombinant human opticin and endogenous rabbit opticin in the vitreous, we developed a selected reaction monitoring mass spectrometry (SRM-MS) method that could distinguish and accurately quantify human and rabbit opticin simultaneously.

MATERIALS AND METHODS

Production of Recombinant Human and Rabbit Opticin. cDNA encoding the mature full-length human or rabbit opticin sequence was cloned into the pCEP-Pu expression vector; this incorporates a BM40 signal peptide which replaces the original opticin signal peptide. The expression vector was transfected into 293-EBNA cells, and cell selection using puromycin was performed as described previously.³ The cells were expanded by culture in Dulbecco's modified Eagle medium containing 10% fetal calf serum, 0.5 $\mu\text{g}/\text{mL}$ puromycin, 100 units/ml penicillin, and 100 $\mu\text{g}/\text{mL}$ streptomycin. Upon confluency, the medium was replaced with Dulbecco's modified Eagle medium without fetal calf serum. After 48 h, the conditioned medium was collected, 5 mM EDTA and 0.5 mM PMSF were added, the medium was then centrifuged to remove debris, and stored frozen.

To purify opticin, the conditioned medium was thawed and mixed with DEAE Sepharose Fast Flow (GE Healthcare) at 4 °C overnight. The DEAE Sepharose was then collected and packed into a column. This column was washed with 50 mM Tris-HCl pH 7.4, 0.15 M NaCl and then eluted with 50 mM Tris-HCl pH 7.4, 0.7 M NaCl. The column eluant was directly applied to a Low Sub Phenyl Sepharose 6 Fast Flow column (GE Healthcare). The column was then equilibrated in 50 mM Tris-HCl, pH 7.4, 0.7 M ammonium sulfate and then eluted using a gradient from 0.7–0 M ammonium sulfate in 50 mM Tris-HCl, pH 7.4. Opticin-containing fractions were then applied to a Dionex Pro Pac SAX-10 anion-exchange column and this was eluted with a gradient of 0–1 M NaCl in phosphate buffer (pH 7.4). Opticin-containing fractions were identified and checked for purity by SDS-PAGE with Coomassie blue staining.

Phase separation with 1% Triton X-114 was used to eliminate any endotoxin contamination from the human opticin.¹⁰ Finally, size-exclusion chromatography was performed in PBS buffer on a Superose 12 10/300 column (GE healthcare). Fractions containing purified, opticin dimer were collected and concentrated using PES protein concentrator spin columns (10K MWCO), and aliquots were fast frozen in liquid nitrogen.

Each batch of produced recombinant opticin was tested using the Limulus amebocyte lysate assay and the Pyros

Kinetix Flex tube reader system (Associates of Cape Cod Incorporated; East Falmouth, MA, U.S.A.) to confirm that it was free from bacterial endotoxin prior to its use in the *in vivo* studies.¹¹

In Vivo Studies. Animal studies were carried out under the Animals (Scientific Procedures) Act 1986 (project license PPL 70/8120, protocol number 8). All procedures were conducted following ethical approval of the Animal Welfare and Ethics Committee of the UCL Institute of Ophthalmology and complied with the ARVO Statement for the Use of Animals in Ophthalmology and Vision Research. Male New Zealand White rabbits were obtained from Envigo (Bicester, U.K.); they were allowed to acclimatize for at least 7 days prior to injection.

A total of 43 eyes were obtained from 22 rabbits weighing 1.4–1.7 kg. Seven eyes were uninjected, and the rest received intravitreal injections. Briefly, the animals were anaesthetised with an intramuscular injection of a mixture of 25 mg/kg ketamine hydrochloride and 0.5 mg/kg medetomidine hydrochloride (Vetoquinol UK Ltd., Towcester, U.K.). In addition, topical anesthesia (1% Tetracaine Hydrochloride ophthalmic eye drops; Bausch&Lomb UK Ltd., Surrey, U.K.) was administered after dilation of the pupils with 1% Tropicamide and 2.5% Phenylephrine hydrochloride eye drops (Bausch&Lomb UK Ltd.). After placing 5% povidone iodine on the periocular region and the conjunctiva of each eye, recombinant human opticin (40 μg in 50 μL total volume; $n = 36$) was administered intravitreally 1 mm behind the surgical limbus of the eye by injection with either a microfine 30-gauge insulin syringe (BD; Franklin Lakes, NJ, U.S.A.) or a 30-gauge needle and a Hamilton syringe (Hamilton Company, Reno, NV, U.S.A.). To manage any possible postoperative pain, injected rabbits received a 5 mg dose of carprofen (administered subcutaneously once a day for 2 consecutive days post intravitreal injection).

The rabbits were sacrificed after intravitreal injection at the following time points: 5, 24, and 72 h and 7, 14, and 28 days by intravenous overdose with pentobarbital sodium (Merial Animal Health Ltd., Harlow, Essex, U.K.). The vitreous was collected from all enucleated eyes by dissection, and it was stored in 1.5 mL eppendorf tubes at -80°C until further analysis. In brief, a small incision in the sclera was made using a scalpel, and the cornea was removed using scissors. The lens was removed and the vitreous collected using a 3 mL Pasteur pipet.

Sample Preparation for Determination of Opticin Concentration. Vitreous samples were thawed to room temperature, and their initial weights were recorded (W_1) prior to 24 h incubation with hyaluronan lyase from *Streptomyces hyalurolyticus* (EC 4.2.2.1; 15 units per sample) at 37 °C with slight agitation (350 rpm). A collagen-containing pellet was separated from the supernatant by centrifugation at 13 000g for 30 min. The supernatant was removed, and a 50 μL aliquot of the supernatant was taken for analysis. The collagen-containing pellet plus tube was reweighed (W_2) before washing with 100 μL of 50 mM ammonium bicarbonate and resuspension in 50 μL of 50 mM ammonium bicarbonate. Both the supernatant and collagen-containing pellet extract were reduced by incubating with 5 mM (final concentration) dithiothreitol at 60 °C for 45 min and subsequently alkylated with iodoacetamide—final concentration 15 mM, at room temperature for 30 min in the dark. Each fraction was next subjected to enzymatic digestion by addition of 2 μg of

proteomics grade trypsin (source Promega, U.K.) to each sample with the volume made up to 93 μL with 50 mM ammonium bicarbonate. Samples were vortexed briefly and incubated for 16 h at either 50 °C (collagen-containing pellet extract) or 37 °C (supernatant) overnight. Two microliters of neat formic acid was added after digestion to inactivate any remaining trypsin.

The optimal peptides were identified following tryptic digestion of purified recombinant human and rabbit opticin. Briefly, recombinant protein was reduced, alkylated, and digested as described above in six technical replicates, and resultant peptides were analyzed by LC-MS on a QStar Elite Q-ToF system as described previously.¹² Data was searched against the relevant species database using MASCOT, and the highest scoring peptides were selected. The extracted ion chromatograph for each peptide was extracted, and peak areas were obtained. The most reproducible peptides were selected as SIS targets. Stable isotope standard (SIS) peptides for selected proteotypic peptides from both rabbit and human opticin were purchased from Thermo Scientific. Peptide identity and purity were confirmed by LC-MS analysis. Peptide sequences are shown in Table 1.

Table 1. Sequences of Proteotypic Peptides Used for the Quantitation of Human and Rabbit Opticin (Heavy Label in Bold)

peptide	amino acid sequence
human - H4	EGDSFEVLPLR
human - H5	LQSSGIQPAAFR
rabbit - R2	AGDFQGLAK
rabbit - R3	LQSSGIQPGAFR
rabbit - R4	TTYLYAR

For vitreous supernatant samples, a stock pool of these peptides was prepared with a final spiking solution concentration of 0.40 pmol μL^{-1} for R2, R3, and R4, and 4.0 pmol μL^{-1} for H4 and H5. For collagen-containing pellet extracts, a separate pool was made with a final spiking solution concentrations of 98.6, 99.4, and 98.8 fmol μL^{-1} for R2, R3, and R4, respectively, and 1000 fmol μL^{-1} for H4 and 990 fmol μL^{-1} for H5.

Five microliters of the mix was added to each digested vitreous sample giving a final sample volume of 100 μL (a 2-fold dilution of the original vitreous material). After the samples were vortexed briefly, they were transferred to LC autosampler vials for subsequent analysis by LC-MS.

Collagen-containing pellet extracts were centrifuged to remove undigested debris, and the supernatant was transferred to an eppendorf tube, and dried down under vacuum. Each sample was resuspended in 10 μL of SIS multimix spiking solution before it was transferred to the LC autosampler vials for subsequent analysis by LC-MS. The original eppendorf tube was rinsed to remove all material, dried, and reweighed (W3) to enable the weights of the collagen-containing pellet and supernatant fraction to be obtained. A summary of the sampling preparation is presented in Supplementary Figure A.

Opticin Determination by SRM-MS. Samples from above were injected (supernatant = 10 μL and collagen-containing pellet extract = 2 μL injection volume) onto an Agilent 1260 Infinity LC system coupled to an Agilent 6495A Triple Quadrupole mass spectrometer operating in SRM acquisition mode. Peptides were separated using a gradient

elution of increasing acetonitrile concentration (Buffer A = Water + 0.1% formic acid, Buffer B = Acetonitrile + 0.1% formic acid) on a C18 column (2.1 mm \times 250 mm, 3 μm , Acclaim 120 – Thermo Scientific, CA, U.S.A.) at a flow rate of 150 $\mu\text{L}\cdot\text{min}^{-1}$. Gradient conditions were, 0–5 min 5% B, 3 min 15% B, 13 min 17% B, 18 min 20% B, 22 min 35% B, 23 min 80% B, 33 min 80% B, 34 min 5% B, 60 min 5% B.

Optimized SRM transitions and collision energies for each light/heavy peptide pair are given, along with expected retention times, in Supplementary Table A.

Prior to each batch of samples, the SIS peptide mix was injected to ensure that the chromatographic retention time and peak widths were appropriate and that the MS signal was as expected to ensure that the system was functioning well.

SRM peak areas were calculated using MassHunter software (version B.08.02) (Agilent Technologies, Santa Clara, CA, U.S.A.) and used to calculate endogenous levels of opticin. The mean concentration obtained for all three transitions was reported. The final human opticin concentrations were calculated from the average concentration of the two peptides for human opticin H4 and H5 from vitreous supernatant (human opticin HOS) and collagen-containing pellet (human opticin HOP). Likewise, rabbit opticin concentrations were the mean of R2, R3, and R4 concentrations in the vitreous supernatant (rabbit opticin ROS) and collagen-containing pellet (rabbit opticin ROP). The calculated concentrations were based upon the monomeric protein sequence; the mature monomeric human protein has a molecular weight of 35.19 kDa, and the mature rabbit sequence has a molecular weight of 32.06 kDa.

Pharmacokinetic Analysis. HOS and HOP were analyzed by a nonlinear mixed-effects (NLME) method using the stochastic approximation expectation maximization (SAEM) algorithm implemented in the MONOLIX software (Monolix version 2019R1. Antony, France: Lixoft SAS, 2019. <http://lixoft.com/products/monolix/>). The concentration data from each eye was treated independently using a naive pool data analysis and one-compartment structural model parametrized with intravitreal volume of distribution (V_{it}) and half-life ($t_{1/2, \text{it}}$). The initial estimates of the parameters were chosen on the basis of the typical values of the intravitreal PK parameters of drugs with similar molecular weight from a comprehensive database.¹³

RESULTS

1. Validation of the Opticin MS Assay. A sensitive mass spectrometry-based assay was developed for the analysis of human and rabbit opticin. Opticin protein levels in vitreous supernatant (HOS and ROS) and in the collagen-containing pellet (HOP and ROP) were simultaneously determined using proteotypic peptides as protein surrogates. Quantitative data were obtained by comparison to spiked synthetic heavy-labeled peptides.¹⁴

Limit of Detection (LOD) and Limit of Quantitation (LOQ). The mass spectrometry signal for a 10 fmol column loading of all five heavy-labeled peptides with all three transitions/peptide overlaid is shown in Figure 1A. From this, it is possible to estimate, on the basis of the signal:noise ratio, a realistic LOD of 1 fmol and LOQ of 3 fmol.

Linearity of Analysis. A calibration series was prepared containing all five heavy peptides with on-column loading ranging from 1 fmol to 10 000 fmol. Each amount was injected in duplicate, and the average peak area for all transitions was

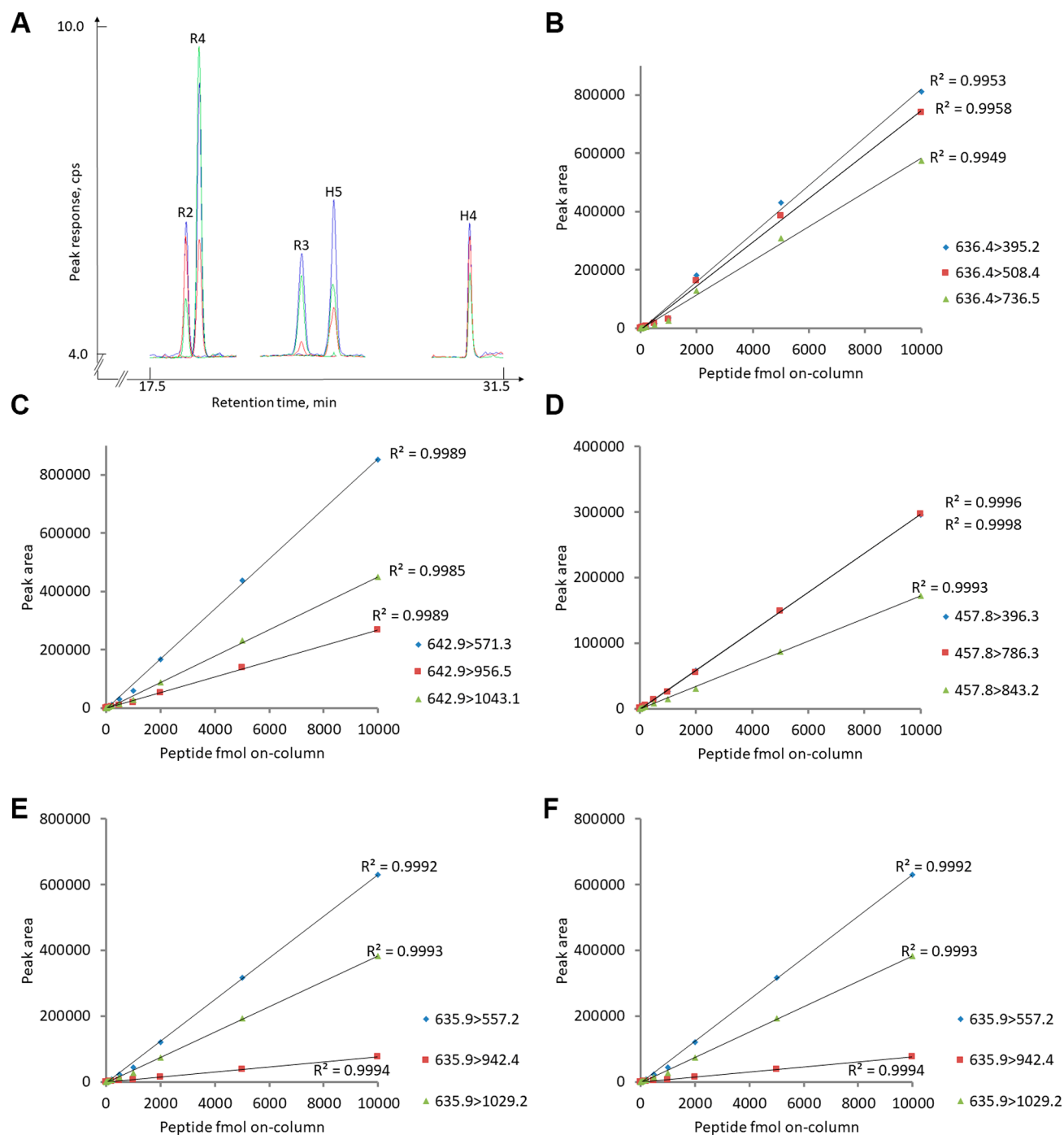


Figure 1. (A) Overlay plot for all SRM-MS transitions of a 10 fmol on-column loading of all five SIS peptides. (B–F) Peptide signal linearity between 1 and 10 000 fmol peptide on-column for the five stable isotope labeled (SIS) peptides; (B) H4, (C) H5, (D) R2, (E) R3, and (F) R4.

plotted against on-column loading (Figure 1B–F). The results of this linearity test clearly demonstrate excellent linearity over 4 orders of magnitude. Log-log linearity data are presented in Supplementary Figure B for clarification.

2. Opticin Concentrations in Vitreous and Pharmacokinetic Analysis. Concentration–time profiles of the four species of opticin HOS, HOP, ROS, and ROP are presented in Figure 2. HOS and ROS represent the concentration of opticin in the vitreous supernatant, after intravitreal injection of 1136 pmol (40 μ g) of human opticin, while HOP, ROP are the corresponding opticin concentrations associated with the collagen-containing pellet during the same time period of the

experiment. For each time point $n = 6$, except for HOP and ROP at time 7 days, and HOS at time 14 days where $n = 5$; the missing data points were due to technical problems.

NLME Model Building of Human Opticin Pharmacokinetics. The structural model used to fit the data was a one-compartmental model of first order elimination from the Monolix library, and it was reparametrized for presenting V_{itv} and $t_{1/2, itv}$ as final parameters using Mlxeditor (see Supporting Information Figure C). The distribution of the PK parameters was set as log-normal, and a correlation between them was selected for the model building.

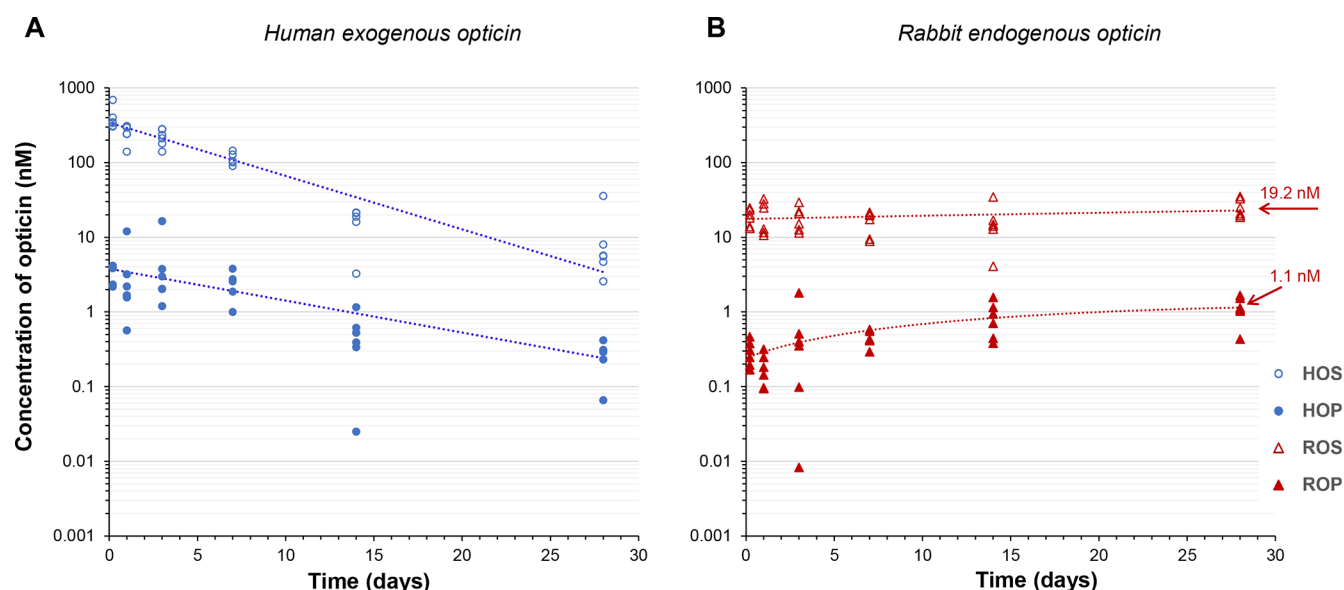


Figure 2. Time–concentration profiles of opticians in rabbit vitreous. (A) The HOS and HOP concentration–time points after a dose of 1,136 pmoles injection. The blue dotted lines correspond to the concentration predictions determined by NLME (the corresponding estimates of the PK parameters are presented in Table 2). (B) The simultaneous concentration levels of rabbit optician ROS and ROP during same time range. The red dotted lines correspond to a linear trendline (MS Excel) for ROS showing a constant level of ROS (with an average concentration of the six time points = 19.2 nM) and the second-order polynomial trendline (MS Excel) for ROP describing low initial levels that increase until the ROP basal typical concentration (concentration at 28 days = 1.1 nM).

The HOS initial estimate for V_{ivt} was 1.5 mL, which correspond to the anatomical volume of rabbit vitreous,¹⁵ and for $t_{1/2, \text{ivt}}$ it was 52 h, which is similar to drugs in the MW range of optician based on the typical values of intravitreal drugs reported earlier.¹³ For HOP, the initial estimates were the parameter estimate values obtained from HOS.

All the concentration–time data ($n = 6-5$) were pooled for the analysis, treating each point as an independent measurement per eye. For this reason, there was no intrasubject variability and so a proportional error model with a fixed value was employed for both drug species (HOS and HOP) (Table 2).

Table 2. Estimated PK Parameters of V_{ivt} and $t_{1/2, \text{ivt}}$ for HOS and $t_{1/2}$ for HOP, with the Corresponding Standard Errors (SE), the Relative Standard Error (RSE %), the Standard Deviation or Omegas of the Estimates, and the Fixed Value Selected for the Proportional Error Model^a

human optician in the supernatant	estimate value	SE	RSE (%)
V_{ivt} of HOS	3.31 mL	0.317	9.6
$t_{1/2, \text{ivt}}$ of HOS	101 h (4.2 days)	8.89	8.8
omega of V_{ivt} of HOS	0.283	0.0827	29.2
omega of $t_{1/2, \text{ivt}}$ of HOS	0.386	0.0688	17.8
proportional error model with a fixed value	0.205		
human optician in the pellet ^a	estimate value	SE	RSE (%)
$t_{1/2, \text{ivt}}$ of HOP	169 h (7 days)	29.6	17.5
omega of $t_{1/2, \text{ivt}}$ of HOP	0.638	0.141	22.2
proportional error model with a fixed value	0.255		

^a V_{ivt} for HOP is not reported because it does not have a physiological meaning.

The injected human optician showed a first-order elimination profile with an intravitreal V_{ivt} of 3.31 mL and $t_{1/2, \text{ivt}}$ of 4.2 days, in the supernatant, and with an intravitreal clearance of 0.023 mL/h calculated based on the equation

$$Cl_{\text{ivt}} = \ln 2 * V_{\text{ivt}} / t_{1/2} \quad (1)$$

The half-life from the pellet data appears to be somewhat longer, 7 days, which might suggest some saturation in the association with the pellet, but with so little associated with the pellet, it is difficult to speculate on the reason for this. The overall fits of HOS and HOP data are summarized by the visual predictive check plot which compares observations and simulations of the model predictions graphically (Figure 3).

Endogenous Rabbit Optician Concentration Analysis. Prior to injection of human optician, the endogenous rabbit optician concentration was measured from the vitreous of seven eyes. The average basal concentrations of rabbit optician in both the vitreous supernatant and collagen-containing pellet were 18.1 and 1.1 nM, respectively, so that 94% of the optician was in the supernatant and only 6% was in the pellet containing the insoluble collagen fibrils. The values are similar to the corresponding ROS and ROP obtained during the PK study shown in Figure 2B. ROS was relatively constant during the experimental period (average concentration of the six time points = 19.2 nM), while ROP levels increase to basal concentrations by the end of the PK study (concentration at 28 days = 1.1 nM). The trendlines presented in Figure 2B aim to describe the tendency of the data without curve fitting purposes. Both plateau and second-order polynomial trends for ROS and ROP respectively were also observed in the arithmetic scale of the plot (data not shown).

Assuming that the constant of elimination is the same for human as for rabbit optician (our hypothesis is that both show the same disposition behavior), the synthesis rate of rabbit optician, ignoring ROP, can be calculated on the basis of the equation below:

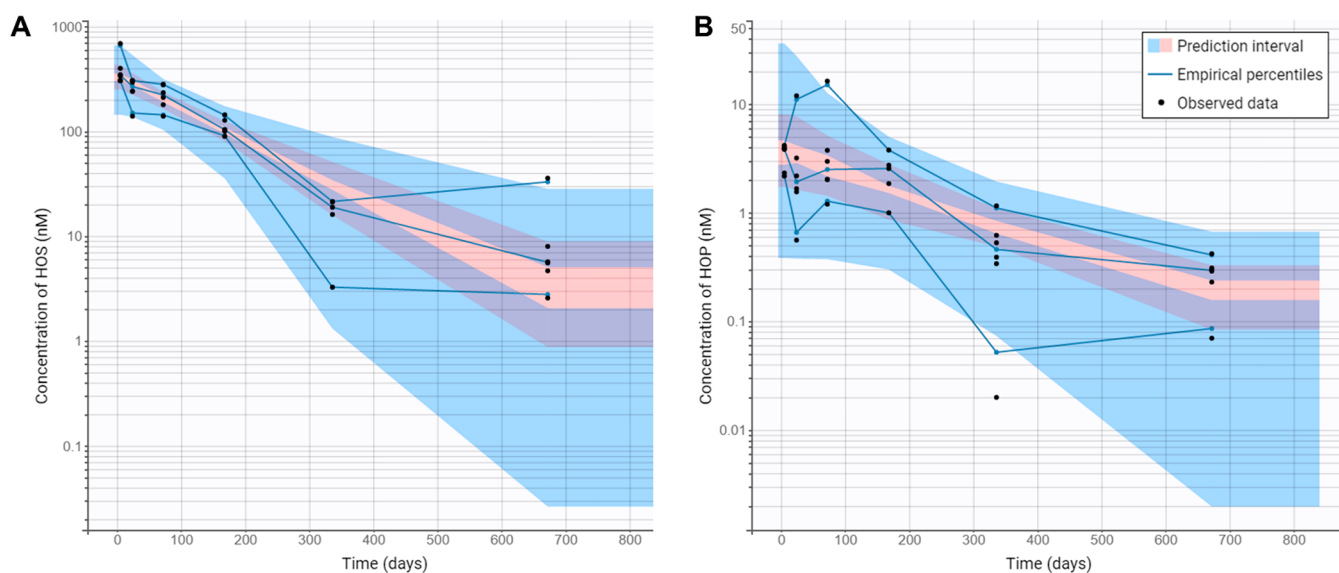


Figure 3. Visual predictive check plots in semilog scale for HOS (panel A) and HOP (panel B) where the solid blue lines represent the empirical percentiles (10%, 50%, 90%) of the observed data (dark dots) which are inside the 90% prediction confidence intervals of the model represented by the blue lower, pink median, and blue upper shaded areas (detailed description of the performance of this plot is in Supporting Information Figure D).

$$\frac{dA_{\text{ROS}}}{dt} = \text{ROS}_{\text{syn}} - k_{\text{el}} \cdot A_{\text{ROS}} \quad (2)$$

where ROS_{syn} is the synthesis rate of rabbit opticin, A_{ROS} is the amount of free rabbit opticin, and k_{el} is the constant of elimination of free rabbit opticin.

The basal concentration of ROS was found to be 18.1 nM. Considering the anatomical vitreous rabbit volume of 1.5 mL¹⁵ and the molecular weight of rabbit opticin of 32.06 kDa, the basal concentration of ROS is 0.58 $\mu\text{g}/\text{mL}$, and the total amount in vitreous is 0.87 μg .

Given that the free human opticin $t_{1/2, \text{ivt}}$ is 4.2 days, from eq 3:

$$k_{\text{el}} = \ln 2 / t_{1/2} \quad (3)$$

k_{el} is equal to 0.165 days^{-1} .

At steady state, ROS_{syn} equals k_{el} times ROS. Therefore, the rate of production of endogenous rabbit opticin is expected to be 0.14 μg of rabbit opticin/day.

The PK profiles in Figure 2 show that HOS reached concentrations of over 24-fold greater than ROS 5 h after injection and then decreased, while ROS remained constant during the experiment. However, after intravitreal injection, there appears to be an interplay between human and rabbit opticin in the collagen-containing pellet. With increased levels of HOP after intravitreal injection, there was an apparent partial replacement of ROP, but this effect was reversed as the human opticin was cleared from the eye, with ROP reaching the preinjection concentration of 1.1 nM by day 28.

DISCUSSION

The primary objective of this study was to characterize the PK profile of human opticin after intravitreal injection into rabbit eyes. The rabbit eye is a good model for intravitreal PK,¹⁶ and because this model has been used to evaluate antiangiogenic molecules in the past, comparisons can be made with pre-existing data.^{17–21} In this study, we measured a $t_{1/2, \text{ivt}}$ of 4.2 days following intravitreal injection of recombinant human

opticin, results similar to 2.88 and 2.75 days for ranibizumab and 3.6 and 4.2 days for aflibercept in the rabbit eye. The V_{ivt} of human opticin is 3.31 mL, 2 times higher than the anatomical volume of rabbit vitreous. Given that the volume of distribution equals the ratio between drug amount in the vitreous and the concentration in the vitreous supernatant, this number shows approximately half of the human opticin is not associated with the vitreous supernatant but bound to other sites. Since the binding to vitreous collagen fibrils was low, the opticin must have bound to other surrounding tissues. Opticin was observed by immunohistochemistry to localize to the basement membranes surrounding the vitreous (i.e., the ILM and lens capsule).⁵ Furthermore, biochemical studies have demonstrated that opticin binds to components of these basement membranes including laminin and type IV collagen.⁸ Therefore, a reasonable explanation is that a significant proportion of the injected opticin was bound to these basement membranes that surround the vitreous.

In order to obtain specific quantitative measurements of the human opticin protein injected into the rabbit eye, we chose to develop an assay based on SRM-MS. The primary driver here was the lack of available antibodies which could reliably distinguish between the rabbit and human forms of opticin, for example, by immunoassay. By contrast, the mass resolving power of MS easily provides the selectivity to distinguish between these two proteins on the basis of the mass differential between tryptic peptides. The assay was optimized using standard analytical workflows.²² Briefly, a list of all theoretical proteotypic peptides for opticin was generated *in silico*, and following the replicated digestion of pure protein, optimum peptides were selected. Selection was based upon the most reproducible yield by MS, generation of at least three strong SRM transitions, and, for the human opticin peptides, the absence of contaminating signal when applied to the analysis of a “blank” matrix (i.e., vitreous samples from an uninjected rabbit eye). The assay was deemed to be specific for the proteins of interest, and we demonstrated that the assay

yielded a linear signal over the required range via a series of standard spike-in experiments.

The overall concentration of endogenous rabbit opticin was found to be 0.62 $\mu\text{g}/\text{mL}$ (19.2 nM). Considering that the anatomical volume of the rabbit vitreous is around 1.5 mL,¹⁵ the total opticin in the rabbit vitreous is estimated to be 0.93 μg . As the amount of injected human opticin was 40 μg , it was approximately 43 times in excess, inducing an apparent partial replacement of rabbit opticin from the collagen fibrils. This effect was reversed as the human opticin was cleared from vitreous.

Collagen fibrils impart a gel-like structure to the vitreous, and opticin was first identified bound to the surface of vitreous collagen fibrils.¹ Centrifugation collapses the vitreous gel with the collagen separating into a pellet from the then-liquid supernatant. Therefore, we separately measured the opticin in the collagen-containing pellet and supernatant to determine what proportion of the total opticin in vitreous was bound to collagen fibrils. Unexpectedly, we found that >90% of the rabbit and injected human opticin were in the supernatant and therefore not bound to the collagen fibrils. Five hours after injection of human opticin, the amount of rabbit opticin in the pellet following centrifugation was lower than normal physiological levels, but this then recovered by day 28; conversely, the amount of human opticin in the pellet was highest at 5 h after injection and lowest at day 28. These data suggest that there may have been some exchange of opticin on the surface of the collagen fibrils, but because the collagen-containing pellet did contain some noncollagenous material, this is a tentative conclusion.

The injected human opticin was cleared from the vitreous, while the concentration of rabbit opticin remained constant during the experiment. Assuming that rabbit opticin is cleared in the same way as the injected human opticin, this implied that new rabbit opticin was being synthesized during the experiment and the rate of synthesis could be calculated. When these calculations were performed a rate of synthesis of rabbit opticin was found to be 0.14 μg opticin/day. As the rabbit vitreous contains a total of approximately 0.93 μg of opticin this implies that there is a remarkable rate of turnover of opticin in the rabbit eye of 15% per day.

Opticin is synthesized by the posterior nonpigmented ciliary epithelium, and this monolayer of cells then secretes it into the vitreous.^{4–6} A broadly held view is that after development, the turnover of extracellular matrix molecules is low. However, using *in situ* hybridization, the expression of opticin mRNA was observed in the adult human posterior nonpigmentary ciliary epithelium, demonstrating active synthesis in the adult eye.⁴ It is unclear why opticin is continually secreted into the vitreous at such a high rate, but this may be important in maintaining the homeostasis of the vitreous and ensuring that it remains avascular, an essential requirement for vision.

CONCLUSIONS

We have determined a volume of distribution of 3.31 mL and half-life of 4.2 days for free human opticin in the rabbit vitreous following intravitreal injection. These values are broadly in the same range as currently available antiangiogenic biological drugs. The total concentration of endogenous opticin in the rabbit vitreous was approximately 0.62 $\mu\text{g}/\text{mL}$; it is the first time this has been quantified in any species. Interestingly, only a small fraction of the rabbit opticin was bound to vitreous collagen fibrils with most of it being present in the vitreous

supernatant. The rate of rabbit opticin synthesis was estimated to be 0.14 $\mu\text{g}/\text{day}$, and remarkably, it is turned over in the vitreous at a rate of 15% per day.

ASSOCIATED CONTENT

Supporting Information

The Supporting Information is available free of charge at <https://pubs.acs.org/doi/10.1021/acs.molpharmaceut.0c00151>.

Supplementary Figure A, a summary of the sampling preparation for the determination of the different opticin species; Supplementary Figure B, log scale linearity of heavy peptides; Supplementary Table A, presenting the optimized SRM transitions and collision energies for each light/heavy peptide pair along with expected retention times; Supplementary Figure C, visual predictive check plots description of the structural model for HOS and HOP in Monolix format, and Supplementary Figure D, visual predictive check plots in linear scale for HOS and HOP, and description of its performance (PDF)

AUTHOR INFORMATION

Corresponding Authors

Paul N. Bishop – Division of Evolution & Genomic Sciences, School of Biological Sciences, FBMH, University of Manchester, Manchester M13 9PL, United Kingdom; Manchester Royal Eye Hospital, Manchester University NHS Foundation Trust, Manchester Academic Health Science Centre, Manchester M13 9WL, United Kingdom; orcid.org/0000-0001-7937-7932; Email: paul.bishop@manchester.ac.uk

Richard D. Unwin – Division of Cardiovascular Sciences, School of Medical Sciences, FBMH, University of Manchester, Manchester M13 9PT, United Kingdom; Stoller Biomarker Discovery Centre and Division of Cancer Sciences, School of Medical Sciences, FBMH, University of Manchester, Manchester M13 9PL, United Kingdom; Email: r.unwin@manchester.ac.uk

Authors

Eva M. del Amo – Division of Pharmacy and Optometry, School of Health Sciences, Faculty of Biology, Medicine & Health (FBMH), University of Manchester, Manchester M13 9PT, United Kingdom; orcid.org/0000-0002-5705-4515

John R. Griffiths – Division of Cardiovascular Sciences, School of Medical Sciences, FBMH, University of Manchester, Manchester M13 9PT, United Kingdom

Izabela P. Klaska – UCL Institute of Ophthalmology, University College London, London EC1V 9EL, United Kingdom

Justin Hoke – UCL Institute of Ophthalmology, University College London, London EC1V 9EL, United Kingdom

Anne White – Division of Evolution & Genomic Sciences, School of Biological Sciences, FBMH, University of Manchester, Manchester M13 9PL, United Kingdom

Leon Aarons – Division of Pharmacy and Optometry, School of Health Sciences, Faculty of Biology, Medicine & Health (FBMH), University of Manchester, Manchester M13 9PT, United Kingdom

Garth J. S. Cooper – Division of Cardiovascular Sciences, School of Medical Sciences, FBMH, University of Manchester, Manchester M13 9PT, United Kingdom

James W. B. Bainbridge – UCL Institute of Ophthalmology, University College London, London EC1V 9EL, United Kingdom

Complete contact information is available at:
<https://pubs.acs.org/10.1021/acs.molpharmaceut.0c00151>

Notes

The authors declare no competing financial interest.

ACKNOWLEDGMENTS

This work was funded by Medical Research Council (MRC), United Kingdom (grant No MR/M025365/1), and facilitated by the Manchester NIHR Biomedical Research Centre and the Greater Manchester Comprehensive Local Research Network. EdA was additionally funded by the European Union's Horizon 2020 research and innovation programme under the Marie Skłodowska-Curie (grant No 799880). J.W.B. was supported by a NIHR Research Professorship.

ABBREVIATIONS

A_{ROS} , amount of rabbit opticin in the supernatant; **HOP**, human opticin in the pellet; **HOS**, human opticin in the supernatant; **ILM**, internal limiting membrane; k_{el} , the constant of elimination; **LOD**, limit of detection; **LOQ**, limit of quantitation; **NLME**, nonlinear mixed-effects; **PK**, pharmacokinetics; **ROP**, rabbit opticin in the pellet; **ROS**, rabbit opticin in the supernatant; ROS_{syn} , the synthesis rate of rabbit opticin; **RSE**, the relative standard error; **SAEM**, stochastic approximation expectation maximization; **SE**, standard errors; **SRM-MS**, selected reaction monitoring mass spectrometry; **SIS**, stable isotope standard; **SLRP**, small leucine-rich repeat proteoglycan/protein; $t_{1/2, ivt}$ intravitreal half-life; V_{ivt} intravitreal volume of distribution; Cl_{ivt} intravitreal clearance

REFERENCES

- (1) Reardon, A. J.; Le Goff, M.; Briggs, M. D.; McLeod, D.; Sheehan, J. K.; Thornton, D. J.; Bishop, P. N. Identification in Vitreous and Molecular Cloning of Opticin, a Novel Member of the Family of Leucine-Rich Repeat Proteins of the Extracellular Matrix. *J. Biol. Chem.* **2000**, *275* (3), 2123–2129.
- (2) Iozzo, R. V.; Schaefer, L. Proteoglycan Form and Function: A Comprehensive Nomenclature of Proteoglycans. *Matrix Biol.* **2015**, *42*, 11–55.
- (3) Le Goff, M. M.; Hindson, V. J.; Jowitt, T. A.; Scott, P. G.; Bishop, P. N. Characterization of Opticin and Evidence of Stable Dimerization in Solution. *J. Biol. Chem.* **2003**, *278* (46), 45280–45287.
- (4) Bishop, P. N.; Takanosu, M.; Le Goff, M.; Mayne, R. The Role of the Posterior Ciliary Body in the Biosynthesis of Vitreous Humour. *Eye* **2002**, *16* (4), 454–460.
- (5) Ramesh, S.; Bonshek, R. E.; Bishop, P. N. Immunolocalisation of Opticin in the Human Eye. *Br. J. Ophthalmol.* **2004**, *88* (5), 697–702.
- (6) Takanosu, M.; Boyd, T. C.; Le Goff, M.; Henry, S. P.; Zhang, Y.; Bishop, P. N.; Mayne, R. Structure, Chromosomal Location, and Tissue-Specific Expression of the Mouse Opticin Gene. *Investig. Ophthalmol. Vis. Sci.* **2001**, *42* (10), 2202–2210.
- (7) Keenan, T. D. L.; Clark, S. J.; Unwin, R. D.; Ridge, L. A.; Day, A. J.; Bishop, P. N. Mapping the Differential Distribution of Proteoglycan Core Proteins in the Adult Human Retina, Choroid, and Sclera. *Invest. Ophthalmol. Visual Sci.* **2012**, *53* (12), 7528–7538.
- (8) Le Goff, M. M.; Sutton, M. J.; Slevin, M.; Latif, A.; Humphries, M. J.; Bishop, P. N. Opticin Exerts Its Anti-Angiogenic Activity by Regulating Extracellular Matrix Adhesiveness. *J. Biol. Chem.* **2012**, *287* (33), 28027–28036.
- (9) Le Goff, M. M.; Lu, H.; Ugarte, M.; Henry, S.; Takanosu, M.; Mayne, R.; Bishop, P. N. The Vitreous Glycoprotein Opticin Inhibits Preretinal Neovascularization. *Invest. Ophthalmol. Visual Sci.* **2012**, *53* (1), 228–234.
- (10) Liu, S.; Tobias, R.; McClure, S.; Styba, G.; Shi, Q.; Jackowski, G. Removal of Endotoxin from Recombinant Protein Preparations. *Clin. Biochem.* **1997**, *30* (6), 455–463.
- (11) Jackie, J.; Lau, W. K.; Feng, H. T.; Li, S. F. Y. Detection of Endotoxins: From Inferring the Responses of Biological Hosts to the Direct Chemical Analysis of Lipopolysaccharides. *Critical Reviews in Analytical Chemistry*; Taylor and Francis Ltd. March 4, 2019; pp 126–137. DOI: 10.1080/10408347.2018.1479958.
- (12) Williamson, A. J. K.; Pierce, A.; Jaworska, E.; Zhou, C.; Aspinal-O'dea, M.; Lancashire, L.; Unwin, R. D.; Abraham, S. A.; Walker, M. J.; Cadecco, S.; et al. A Specific PTPRC/CD45 Phosphorylation Event Governed by Stem Cell Chemokine CXCL12 Regulates Primitive Hematopoietic Cell Motility. *Mol. Cell. Proteomics* **2013**, *12* (11), 3319–3329.
- (13) Del Amo, E. M.; Vellonen, K. S.; Kidron, H.; Urtti, A. Intravitreal Clearance and Volume of Distribution of Compounds in Rabbits: In Silico Prediction and Pharmacokinetic Simulations for Drug Development. *Eur. J. Pharm. Biopharm.* **2015**, *95*, 215–226.
- (14) Kirkpatrick, D. S.; Gerber, S. A.; Gygi, S. P. The Absolute Quantification Strategy: A General Procedure for the Quantification of Proteins and Post-Translational Modifications. *Methods* **2005**, *35* (3), 265–273.
- (15) Green, H.; Sawyer, J. L.; Leopold, I. H. Elaboration of Bicarbonate Ion in Intraocular Fluids: II. Vitreous Humor, Normal Values. *AMA Arch. Ophthalmol.* **1957**, *57* (1), 85–89.
- (16) del Amo, E. M.; Urtti, A. Rabbit as an Animal Model for Intravitreal Pharmacokinetics: Clinical Predictability and Quality of the Published Data. *Exp. Eye Res.* **2015**, *137*, 111–124.
- (17) Bakri, S. J.; Snyder, M. R.; Reid, J. M.; Pulido, J. S.; Ezzat, M. K.; Singh, R. J. Pharmacokinetics of Intravitreal Ranibizumab (Lucentis). *Ophthalmology* **2007**, *114* (12), 2179–2182.
- (18) Christoforidis, J. B.; Williams, M. M.; Kothandaraman, S.; Kumar, K.; Epitropoulos, F. J.; Knopp, M. V. Pharmacokinetic Properties of Intravitreal I-124-Aflibercept in a Rabbit Model Using PET/CT. *Curr. Eye Res.* **2012**, *37* (12), 1171–1174.
- (19) Ahn, S. J.; Ahn, J.; Park, S.; Kim, H.; Hwang, D. J.; Park, J. H.; Park, J. Y.; Chung, J. Y.; Park, K. H.; Woo, S. J. Intraocular Pharmacokinetics of Ranibizumab in Vitrectomized versus Non-vitrectomized Eyes. *Invest. Ophthalmol. Visual Sci.* **2014**, *55* (1), 567–573.
- (20) del Amo, E. M.; Rimpelä, A. K.; Heikkinen, E.; Kari, O. K.; Ramsay, E.; Lajunen, T.; Schmitt, M.; Pelkonen, L.; Bhattacharya, M.; Richardson, D.; et al. Pharmacokinetic Aspects of Retinal Drug Delivery. *Prog. Retinal Eye Res.* **2017**, *57*, 134–185.
- (21) Park, S. J.; Oh, J.; Kim, Y. K.; Park, J. H.; Park, J. Y.; Hong, H. K.; Park, K. H.; Lee, J. E.; Kim, H. M.; Chung, J. Y.; et al. Intraocular Pharmacokinetics of Intravitreal Vascular Endothelial Growth Factor-Trap in a Rabbit Model. *Eye* **2015**, *29* (4), 561–568.
- (22) Blankley, R. T.; Fisher, C.; Westwood, M.; North, R.; Baker, P. N.; Walker, M. J.; Williamson, A.; Whetton, A. D.; Lin, W.; McCowan, L.; et al. A Label-Free Selected Reaction Monitoring Workflow Identifies a Subset of Pregnancy Specific Glycoproteins as Potential Predictive Markers of Early-Onset Pre-Eclampsia. *Mol. Cell. Proteomics* **2013**, *12* (11), 3148–3159.